Supercritical Fluid Extraction of Packed Beds: External Mass Transfer in Upflow and Downflow Operation

Frank Stüber, Ana Ma. Vázquez, Ma. Angels Larrayoz, and Francesc Recasens*

Department of Chemical Engineering, ETS d'Enginyers Industrials de Barcelona, Universitat Politècnica de Catalunya, Diagonal 647, 08028 Barcelona, Spain

The effects of flow direction of solvent (CO_2) on the fluid-to-particle mass transfer were studied for packed beds of sintered porous pellets of two sizes (diameters of 1 and 2 cm) at conditions supercritical with respect to carbon dioxide using toluene and 1,2- dichlorobenzene as the impregnating solutes. Dynamic extraction experiments were performed in the laminar flow regime ($Re = 8-90$) where both free and forced convection modes of mass transfer were found to be significant. Measured mass transfer coefficients showed an almost linear dependence on the Reynolds number ($Re^{\approx 0.9}$). Downflow of fluid had a strong effect on accelerating extraction rates, in particular at lower Reynolds numbers and for conditions near the critical point of CO_2, where natural convection is dominant. Experimental mass-transfer coefficients were well correlated using a single general equation that accounts for both modes of mass transfer (free and forced convection) as well as for upflow or downflow operation (i.e., with gravity opposing or assisting forced convection).

Introduction

During the last decades, supercritical fluid extraction (SCFE) has been successfully applied as an alternative to conventional separation methods in the chemical, food, pharmaceutical, biochemical, and environmental industries (McHugh and Krukonis, 1994). SC fluids often prove to be efficient extractants with better transport properties (diffusivity, mass transfer coefficient, penetration ability) than most commonly employed liquid solvents. When using carbon dioxide as a fluid (critical temperature, 304.1 K; critical pressure, 7.38 MPa), further advantages are the energy savings and the reduction of degradation of temperature-sensitive substances, as well as the advantages derived from its nonflammability, nontoxicity, easy regeneration, and commercial availability.

So far, a relatively large number of thermodynamic and phase equilibrium studies have been carried out (Brennecke and Eckert, 1989). By contrast, mass-transfer studies are very scarce (Brunner, 1995). Only a few studies are available on intraparticle or effective diffusivities and external fluid-to-solid mass-transport coefficients. Due to a lack of mass-transfer correlations, authors (Brunner, 1985; Recasens et al., 1989; Jones, 1991; Madras et al., 1994) have been obliged in the past to use existing low-pressure correlations such as that of Wakao−Kaguei (1982), which may not apply for packed beds with SCFs. A detailed review of experimental conditions and existing mass transfer correlations is available (Puiggené, 1996).

All authors generally coincide in concluding that depending on system conditions, (pressure, temperature, flow rate), the prevailing mass-transport mechanism in SCFE can be considerably affected by natural convection. This was pointed out early theoretically and proved experimentally by Debenedetti and Reid (1986). Conditions near the critical point favor natural convection since fluid viscosities are anomalously small, while densities are very large. This leads to significant Grashof numbers (10^7-10^9), even for small density gradients between the pure bulk fluid and the saturated solute−fluid mixture. As reasoned by Debenedetti and Reid (1986), in mass-transfer correlations developed for SCFs, the Grashof number must be considered, as done by Lim et al. (1989, 1990, 1994), Lee and Holder (1995), and Puiggené (1996).

From an engineering point of view, the influence of free convection suggests that by operating the extractor with downflow of fluid, advantage could be taken from the enhancement in mass transfer due to gravity in order to shorten extraction times of a separation process. However, it is surprising that up to now, there exist only a few studies comparing the performance of gravity-affected flows in SCFE. Thus, Beutler et al. (1988a,b) often found the rate of oil extraction at SC conditions to be accelerated by gravity-assisted solvent flow (downflow) when compared to gravity-opposed (upflow) solvent flow. A similar phenomenon was observed by Barton et al. (1992) in a work about extraction of peppermint oil with SC CO_2. Sovová et al. (1994), studying the SCFE extraction of grape oil from milled seeds, reported that upflow extraction was retarded due to free convection. The smaller the amount of milled seeds in the extractor and the slower the upward (opposing) flow rate, the more pronounced was this effect. Evaluation of mass-transfer coefficients in the SC phase from extraction curves using a plug flow model shows that the product, $k_f a_0$, is twice as large in runs with downflow of solvent compared to the upflow mode (Sovová et al., 1994).

The only systematic investigation on the effect of flow direction in SCFs has been carried out by Lim et al. (1994) using two different gas−solid systems (naphthalene−CO_2 and benzoic acid−CO_2) under sub- and supercritical conditions. They noted, by comparing experimental data, that (1) the case of gravity-assisting flow tends to enhance mass transfer in both gas−solid systems and, (2) the effect of natural convection is most important in the vicinity of the critical point of CO_2. The authors propose a semiempirical equation correlating their data of mixed forced and natural convection according to the cubic combination rule due to Churchill (1977) for heat transfer, first applied by Knaff and Schlünder (1987) to SCF systems; i.e.,

$$Sh_T^3 = |Sh_F^3 \pm Sh_N^3| \qquad (1)$$

where the minus sign is for opposing flows and the plus

S0888-5885(96)00151-0 CCC: $12.00

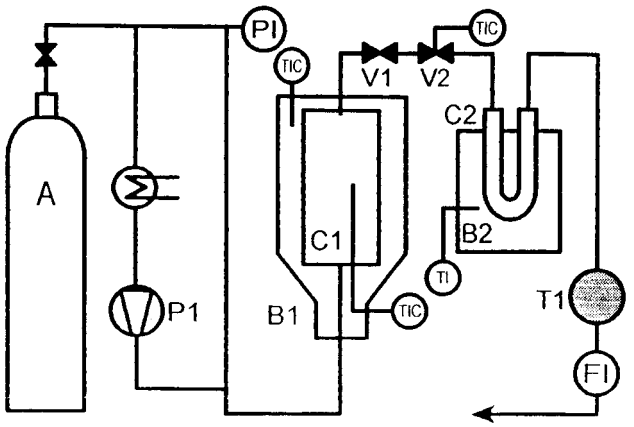

Figure 1. Experimental setup.

sign for assisting flows. In eq 1, $Sh_N = m_2(ScGr)^{1/4}$, and $Sh_F = m_1Re^{0.5}Sc^{1/3}$. To better fit all the experimental results, Lim et al. (1994) used different optimal values for the coefficients m_1 and m_2 for assisting and opposing flows. But as the differences in the parameters are small, their work indicates that except for the plus or minus sign, one single equation such as eq 1 would fit both upflow and downflow data. We prove this in the present paper.

The objective of this work was to investigate the influence of the flow direction of solvent on the external mass-transfer coefficient in fixed beds of solid particles. Systems other than the classical naphthalene−CO_2 were examined. We study the systems of 1,2-dichlorobenzene−CO_2 and toluene−CO_2. Further parameters studied were pressure, temperature, fluid velocity, and pellet size. The data are used as a basis to develop a general mass transfer correlation by considering both free and forced convection with a suitable combination rule. Such correlations are useful in predicting mass-transfer rates in the design of extractors and adsorbers in the presence of gravity effects.

In the experiments, we used macroporous metal cylinders of two sizes (1- and 2-cm equivalent diameters). In order to establish pellet-to-fluid mass-transfer coefficients, the initial extraction rates of the impregnated particles are measured. When porous pellets are put in contact with SC carbon dioxide, a possible mechanism of extraction is capillary action (Barton et al., 1993). CO_2 dissolves into the liquid, leading to a reduction in density and viscosity. This forces the liquid out from the pores and to overflow on the external surface, thus increasing the area for mass transfer. In the present work, we consider the indetermination in the effective area due to of this capillary effect.

Experimental Section

A schematic diagram of the experimental apparatus is shown in Figure 1. Liquid carbon dioxide (SCF chromatography grade, Carburos Metálicos, Barcelona) was compressed by a double-head, steel diaphragm pump (P1) and fed into the system. A heat exchanger (operated at $T = 275$ K) was used to cool the suction stream to the pump. Pressure oscillations were damped by a back-pressure control valve which allowed excess liquid solvent to recirculate to the suction side. System pressure was maintained to within ±1% of the desired value. The pressurized solvent flows either upflow or downflow into the cylindrical high presssure extractor (0.03-m i.d., 0.255 m long, wall thickness of 0.011 m). The extractor temperature was regulated by a heating device, and temperatures measured inside the extractor

Table 1. Experimental Conditions

T	310−360 K
P	8−20 MPa
v_{SCF}[a]	$(0.6-6.7) \times 10^{-4}$ m/s
Sc	1.5−10
Gr	$(0.35-20) \times 10^8$
Re	8−90
solutes used for extraction	toluene and 1,2-DCB
amt of solute or charged per run,[b] kg	
small pellets	0.024 (DCB) and 0.0016 (toluene)
large pellets	0.038 (DCB)

	small pellet packing	large pellet packing
height, H, m	0.02[c]	0.05[d]
cross section, S, m^2	7×10^{-4}	7×10^{-4}
a, m^2/m^3	89	17
d_pL_p, m	0.008 × 0.0082	0.02 × 0.0116
d_{eq}, m	0.01	0.02
θ_{pellet}	0.205	0.25

[a] v_{SCF}, supercritical velocity at supercritical conditions. [b] Amount of solute charged per run is 5% more. [c] Two layers. [d] Three single-particle layers.

(thermocouple type J) indicated fluctuations of ±0.5 K. The fluid pumping unit and the extractor cell are special designs of Marc Sims SFE (Berkeley, CA).

The extractor cylinder was normally filled with small or large cylindrical pellets which were placed between sections of inert packing (1-mm-diameter glass beads and glass wool). The fluid mixture leaving the extraction cell was continuously passed through a shut-off valve (V1) and expanded to atmospheric pressure into an U-tube through a heated ($T = 373$ K) metering valve (V2). The actual flow rate was controlled by the metering valve (V2) and measured in a rotameter (F1). The total amount of CO_2 passed through the system was measured with a calibrated wet-testmeter (T1). Special care was taken so that the dead volume between cell exit and valve V2 is small, as required by the dynamic nature of the experiments. The dead volume, determined by water displacement, amounted to 1.8 cm^3. Separation of solute and solvent was carried out in the U-tube, immersed in pelletized dry ice. The inlet and oulet of the U-tube were packed with 5-cm-long sections of glass wool to obtain complete separation of solute and solvent. Extraction runs were performed using two different solutes, toluene and 1,2-dichlorobenzene (DCB), impregnated on macroporous metallic pellets (steel cylinders of 8-mm diameter × 8.2-mm length and bronze cylinders of 20 mm diameter × 11.6 mm length). The pellets were prepared by a powder-sintering process at AMES (Barcelona), with defined porosity. Prior to extraction experiments, the pellets were impregnated with either DCB or toluene. Simple impregnation by submerging the small pellets in solute at room temperature over 24 h gave good results. On the other hand, the large pellets had to be impregnated under vacuum to completely fill the pores with liquid solute (AMES impregnating methodologies). Typical extraction weights in an experimental run were 2.4 g for small pellets (20 pellets per run) and 3.8 g for large pellets (3 pellets per run) in the case of DCB. All the characteristics and specifications of pellets, bed packings, solvent, and solutes used are summarized in Table 1. For each experimental run, the extractor was preheated close to the desired temperature and then filled with the preweighed pellets. Carbon dioxide was pressurized to the operating pressure by the liquid pump. In this way, the time the system needs to reach pressure and thermal equilibrium was shortened to about 1−3 min depending on the operating pressure. At zero time, the shut-off

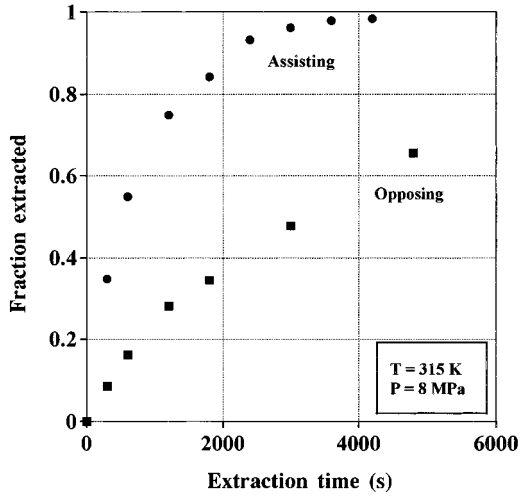

Figure 2. Extraction runs for DCB with upflow and downflow operation.

valve (V1) was fully opened and the flow rate was set with the metering valve (V2) and the rotameter (F1). Depending on the operating conditions and progression of extraction, about 10−15 intermediate samples were taken at 0.5−20-min intervals by closing V2. Three different U-tubes used in the rotation reduced the standby of extraction to a short period necessary to change U-tubes. The weight of the condensate in the tared U-tubes was measured with a digital balance (±0.01*g*). Solute recovery is usually better then 93−95 wt % when based on the total amount of extract determined by weighing the pellets before and after the extraction. Runs which gave solute recoveries smaller than 90 wt % were discarded and repeated. Mass fraction vs time curves are generally composed of a linear initial part (fast extraction) and a very flat end tail (slow extraction) connected by a transition section, as can be seen in Figure 2.

Replicate runs at different conditions were performed but with less intermediate samples. The reproducibility of extraction was excellent. Also, the number of intermediate samples or the standby apparently does not affect the course of extraction. Thus, we can conclude that the present experimental setup and procedures are suitable to determine mass-transfer coefficients in fixed beds from sharply defined initial rates of extraction. The ranges of operating parameters examined in this study are given in Table 1.

Determination of Mass-Transfer Coefficients

In this study, external mass-transfer coefficients for packed beds of porous particles are determined from initial rates of extraction. Consider a differential bed of equally sized porous pellets impregnated with solute to be extracted. At time $t = 0$, and only at this time, the pellets can be treated as quasi-nonporous since diffusional resistances in the pores are still negligible, as they are completely filled with liquid. Assuming pressure, temperature, and flow rate to be constant, the conservation of solute at $t = 0$ leads to the following equation:

$$-\frac{\mathrm{d}m}{\mathrm{d}t} = K_G a_{\mathrm{eff}}(C^*_G - C_G)VM_{\mathrm{solute}} \qquad (2)$$

where K_G is the overall gas-phase mass transfer coefficient based on effective mass-transfer area a_{eff}. The effective area a_{eff} is likely to vary during the extraction process, because capillary drying (Barton et al., 1993) may significantly increase the effective area by wetting a portion of the external pellet surface during the initial extraction period.

Table 2. Solubility of 1,2-Dichlorobenzene in SC CO_2 at $T = 310$ K

P, MPa	10^3K^{exp} [a]	10^3K^{cal} [a]	10^3K^{cal} [a]	C^*_G,[b] mol/m^3	Y^*,[b] mol/mol
8	28	7	18	51	0.004 48
9	95	49	80	360	0.023 88
10	88	67	92	490	0.030 54
16.5	145	120	201	1050	0.057 82
25.5	215	222	340	1631	0.087 11

[a] Puiggené, 1996 ($k_{12} = 0.1275$). [b] Calculated with $k_{12} = 0.1175$ using the PR EOS.

For a shallow or a differential bed (i.e, for small residence times), $C_{G(t=0)} = 0$ is a reasonable approximation. Hence, referring the effective area (a_{eff}) to the total external surface area of pellets (a), a modified mass transfer coefficient, K_G', can be evaluated using the above equation as

$$K_G' = K_G\frac{a_{\mathrm{eff}}}{a} = \frac{-(\mathrm{d}m/\mathrm{d}t)_{t=0}}{aC^*_G VM_{\mathrm{solute}}} \qquad (3)$$

where the numerator is the initial slope of the extraction curve, V is the total bed volume, M_{solute} is the molar weight of solute, and C^*_G is the concentration of solute in the fluid at saturation or its solubility at the selected operating conditions.

As pointed out earlier, a_{eff} may undergo changes due to the effect of capillary drying in the initial extraction period. When carbon dioxide is dissolved in the organic phase contained in the pores, the solution may swell and spread over the external surface of the porous pellets, where it is subject to evaporation into the carbon dioxide rich phase. After a certain fraction of the liquid is extracted, the surface is no longer wetted, the extraction rate slows down, and diffusion in the pores becomes dominant.

To check the effect of capillary drying, Figure 2 shows extraction runs at $P = 8$ MPa, $T = 315$ K, low Reynolds number, and different modes of operation, i.e., downflow and upflow. At these conditions, the changes between the initial extraction period and the transition to the diffusion period are clearly seen. Assuming no change of K_G and the driving force at the inflection point, the ratio r of the slopes of the initial period (with completely wetted pellets) and the pore diffusion step should match the reciprocal value of pellet porosity, i.e., a value of 5 for the small pellets. As can be seen in Figure 2, the calculated values of r vary from 3.1 (315 K, upflow) to 8.7 (315 K, downflow). It is difficult to relate these values as well as the variation of r only to the presence of capillary drying. A more important change of K_G basically due to the effect of natural convection may give a better explanation for the observed results. However, it seems impossible to correctly determine a_{eff}, due to the hypothesis of capillary drying effects. Thus, we referred the effective area to the total external surface area of pellets to calculate the values of the overall gas-phase mass-transfer coefficient K_G'.

Evaluation of equilibrium and transport data for pure substances and mixtures in SCF work usually involves precise knowledge of material properties and usage of estimation methods. In the Appendix, we briefly refer to the methods employed. In Table 2, the solubilities of DCB in SC CO_2 are given. They were necessary to calculate the denominator of eq 3.

Table 3. Operating Conditions for Runs in the (A) Upflow Mode and (B) Downflow Mode

P, MPa	T, K	ρ_{SCF}, kg/m^3	μ_{SCF}, 10^5 Pa s	D_M, 10^8 m^2/s	$\Delta\rho/\rho^*$	C^*_G, mol/m^3	v_{SCF}, 10^4 m/s	Re	Sc	$10^{-8}Gr$	Sh_{exp}
					(A) Upflow						
8.5	315	324	2.5	3.33	0.0970	30.88	1.8	23.7	2.32	1.66	5.78
8.2	311	350	2.78	3.03	0.2391	77.50	3.5	45.8	2.6	4.53	9.68
8.1	310	355	2.8	2.98	0.3401	100.6	6.6	82.4	2.65	7.65	15.56
8	333	192	1.96	5.79	0.0665	9.8	3.1	30.1	1.77	0.625	7.11
8	350	164	1.88	6.98	0.0479	11.8	3.8	32.2	1.64	0.353	5.45
12	323	576	3.94	1.73	0.1076	327	0.99	14.22	3.9	2.38	2.65
12.5	326	570	3.79	1.77	0.1049	323	1.3	19.38	3.76	2.45	3.36
11.5	323	540	3.59	1.89	0.1107	259	2.7	36.9	3.52	2.55	6.89
12.5	324	598	4.17	1.65	0.1058	377	3.5	49.8	4.23	2.25	8.08
11.5	321	583	4.12	1.69	0.1112	334	4.5	62.5	4.2	2.31	12.88
12.5	323	612	4.39	1.59	0.1054	404	5.2	71.7	4.5	2.11	12.53
11.75	315	676	5.6	1.33	0.0987	537	3.1	33.1	6.23	1.47	5.92
12.75	333	504	3.16	2.12	0.0902	212	4.2	65.55	2.96	2.33	13.01
20	315	830	7.16	0.93	0.1098	1256	0.67	7.7	9.24	1.53	1.29
20	335	711	5.4	1.31	0.1291	957	0.79	10.2	5.81	2.38	1.82
19	316	811	6.96	0.95	0.1093	1169	1.87	21.5	8.88	1.55	3.44
19	317	814	6.91	0.97	0.1115	1160	3.44	39.7	8.71	1.61	6.58
					DCB−Large Pellets						
20.5	314	840.5	7.32	0.906	0.126	1300	0.98	24.1	9.61	14.5	9.02
20	318	811	6.94	0.986	0.139	1232	1.82	44.0	8.67	16.5	12.40
20.5	315	832.5	7.21	0.928	0.128	1289	2.69	64.7	9.33	14.9	16.51
					Toluene−Small Pellets						
9.2	328	267.5	2.2	4.56	0.144	122	1.09	13	1.8	2.25	2.01
9.2	323	302	2.34	3.98	0.249	190	1.60	20.2	1.95	5.1	3.89
9.2	323	302	2.34	3.98	0.249	190	2.89	36	1.95	5.1	7.79
9.2	324	298	2.32	4.04	0.181	156	6.25	78.7	1.93	3.37	13.62
					(B) Downflow						
8.5	313	450	3.467	2.285	0.2707	221	1.32	16.8	3.4	5.66	7.13
8.5	314	343	2.650	3.124	0.0873	36	4.30	54.7	2.47	1.73	16.56
8.5	310.5	479	3.697	2.115	0.2479	249	6.68	82.4	3.64	5.11	26.7
12	322.5	576	3.970	1.734	0.1069	326	0.96	13.1	4.25	2.33	6.05
12	323.5	605	4.320	1.620	0.1057	391	2.41	35.6	3.97	2.34	13.05
12	320	629	4.810	1.514	0.1057	488	4.21	54.0	5.05	1.86	17.51
20	312.5	844	7.358	0.896	0.1172	1343	0.66	7.40	9.75	1.66	4.14
20	313	841	7.321	0.903	0.1072	1271	1.66	18.7	9.64	1.46	6.92
20	312.5	844	7.358	0.896	0.1172	1343	3.31	37.2	9.75	1.61	12.4
					DCB−Large Pellets						
19.5	322	785	6.63	1.06	0.1361	1134	0.97	23.9	7.97	16.6	15.01
19	317	809	6.91	0.99	0.1282	1157	1.79	43.0	8.66	15.3	16.9
21	315.5	837	7.28	0.92	0.1241	1316	2.60	62.3	9.47	14.3	19.8
20	333	724	5.644	1.262	0.1324	996	1.99	52.9	6.18	21.4	20.6
					Toluene−Small Pellets						
9.2	323	302	2.31	3.98	0.2490	190	1.25	15.8	1.90	5.10	6.4
9	322.5	285	2.27	4.20	0.1931	136	2.95	35.8	1.96	5.11	12.83
9	326	260	2.23	4.26	0.2011	120	5.89	68	2.01	3.15	16.15

Results and Discussion

Extraction curves are used to illustrate the effects of operating variables (temperature, pressure, particle size, fluid velocity and flow direction) on the initial rates of extraction of packed beds of porous pellets. Detailed information on operating conditions property data, and resulting Sh numbers for all runs are given in Tables 1 and 3.

Effect of Temperature. Figure 3 shows the initial extraction curves of DCB for a bed of small pellets as a function of temperature and three different pressures for upflow operation (gravity-opposing flow).

At lower pressure (8 MPa) and quasi-constant Reynolds number, the upper curves on Figure 3 reveal a retrograde behavior, a phenomenon also observed in the SCFE of substances retained on adsorbents (Tan and Liou, 1988), as well as for pure solids (Kelley and Chimowitz, 1990; Recasens et al., 1993). An increase in the extraction temperature of 20 K initially decreases the extraction rate, whereas a higher temperature increment has only a minor effect. Solubility data calculated at given operating conditions perfectly reflect the same trend. The initial solubility at 315 K (with a solubility of $C^*_G = 31$ mol/m^3) drops 3 times when the temperature is 336 K ($C^*_G = 10$ mol/m^3) and remains invariable at $T = 355$ K ($C^*_G = 11$ mol/m^3). The negative effect of the retrograde solubility on extraction rate is partially compensated by a 2-fold increase in diffusivity of DCB in SC CO_2 in the temperature range of 336−355 K.

At intermediate pressure (12 MPa, middle curves in Figure 3), variation of the extraction rate with temperature becomes very small. Then, at 20 MPa, it is slightly positive (see bottom curves, Figure 3). In a related work (Puiggené, 1996), the same behavior was observed using the same liquid−fluid system but with a bed of nonporous spheres covered by liquid DCB. Those results and our data lead to the conclusion that the system DCB−CO_2 has a crossover pressure that is likely within 15−20 MPa, depending on temperature.

Effect of Pressure. As observed by different authors (Lim et al., 1990, 1994; Puiggené, 1996), increasing the pressure results in higher initial extraction rates. It is interesting to note that our results indicate a strong, roughly linear dependence of extraction rate on solubility and on pressure. For example, at constant Reynolds number and the same extraction time, the extracted mass fractions of DCB as well as calculated values of

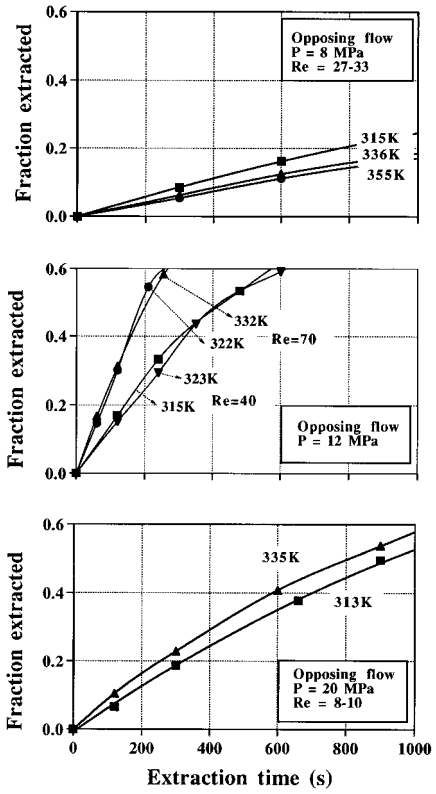

Figure 3. Effect of temperature on the extraction of DCB from small pellets at constant pressure (upper curve 8 MPa and bottom 20 MPa) for opposing flow.

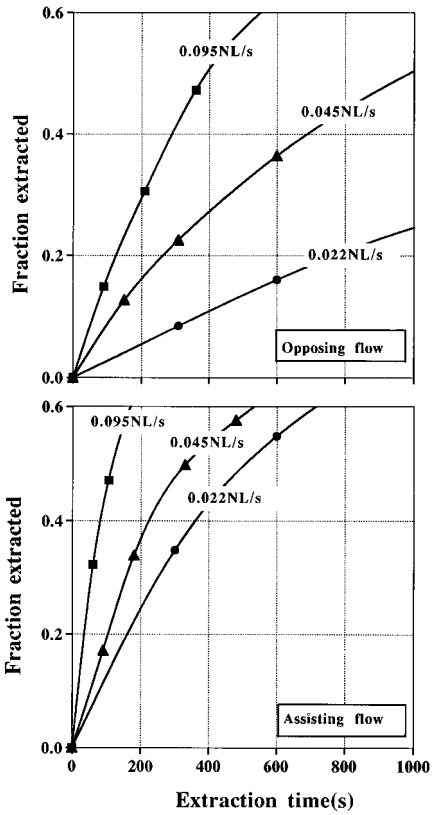

Figure 4. Effect of CO_2 flow rate and flow direction on the extraction of DCB from small pellets at low pressure (8 MPa) and 323 K. NL/s = L/s at 20 °C, 1 atm.

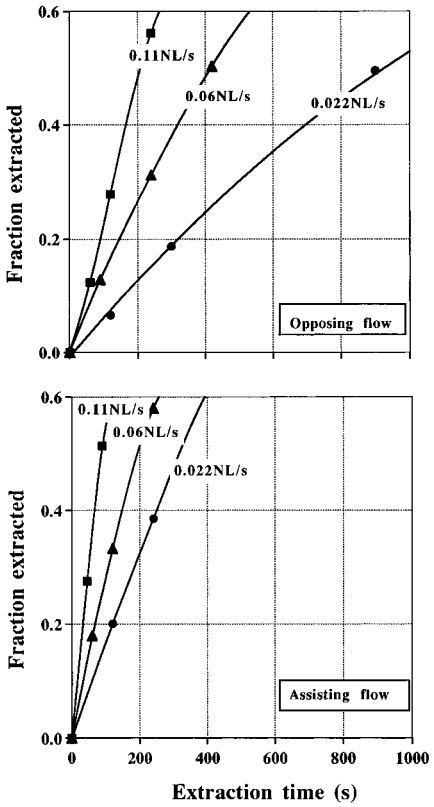

Figure 5. Effect of CO_2 flow rate and flow direction on the extraction of DCB from small pellets at high pressure (20 MPa) and 313 K. NL/s = L/s at 20 °C, 1 atm.

solubility and diffusivity are as follows: $X = 0.08$ at 8 MPa ($C^*_G = 78$ mol/m^3, $D = 3.03 \times 10^{-8}$ m^2/s), $X = 0.33$ at 12 MPa ($C^*_G = 540$ mol/m^3, $D = 1.33 \times 10^{-8}$ m^2/s), and $X = 0.61$ at 20 MPa ($C^*_G = 1160$ mol/m^3, $D = 0.97 \times 10^{-8}$ m^2/s). As is noted, the extraction rate is very sensitive to pressure in the vicinity of the critical pressure of CO_2 compared to pressures close to the crossover pressure. Solubility can thus be identified as one of the key parameters for characterizing the extraction of DCB with SC CO_2.

Effect of Flow Rate and Flow Direction. Experimental runs were performed at various flow rates, different pressures, and constant temperatures and with fluid flowing in a direction opposite to gravity (upflow mode) and in its direction (downflow or assisting mode). For the extraction of DCB from small pellets, Figures 4 and 5 illustrate the initial rates at 8 and 20 MPa, for upflow and downflow operation. Table 4 (and Figure 6) gives the corresponding values of $t_{50\%}$ (time necessary for 50% extraction of solute) for both directions of flow. Two conclusions can be drawn. (1) Regardless of flow direction, the rate increases strongly, almost linearly, with flow rate. Besides solubility, external mass transfer (particularly particle-to-fluid) must be considered to be an important parameter of the system. (2) Despite the strong dependence on flow rate, gravity-assisting flow enhances the extraction rate significantly (see Figures 4 and 5). This effect appears to be more pronounced at low Reynolds numbers and at pressures closer to the critical pressure of CO_2 (see Figure 6 and Table 4). This behavior is certainly related to the presence of free convection and has been noted by other authors (Debenedetti and Reid, 1986; Lim et al., 1990, 1994; Lee and Holder, 1995; Puiggené, 1996). Apparently, extraction runs are performed in the regime where both free and forced convection determine mass transfer. Experiments carried out with other systems (DCB−CO_2−large pellets, toluene−CO_2−small pellets) confirm this observation.

The enhancing effect of gravity in accelerating extraction is most interesting from a practical industrial point of view. Extraction rates may be considerably increased

Table 4. Extraction Times for 50% Recovery of Solute

P, MPa	T, K	Re	$(t_{50\%})_{opp}$, min	Re	$(t_{50\%})_{ass}$, min	E^a
8	313	24	52	17	8.3	6.3
		46	17.2	55	5.5	3.1
		82	7.2	82	2.5	2.9
12	323	14	17.5	13	8	2.2
		40	8.3	36	3.1	2.6
		63	3.5	54	2.2	1.6
20	311	8	15	8	5.3	2.8
		22	7.1	19	3.1	2.3
		40	3.5	34	1.6	2.2

[a] $E = (t_{50\%})_{opp}/(t_{50\%})_{ass}$.

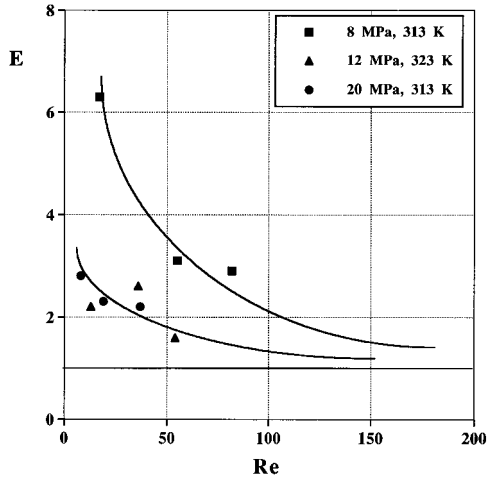

Figure 6. Ratio (E) of extraction times for 50% recovery for upflow and downflow vs Reynolds number, far from the critical point (bottom curve) and near the critical point (upper curve). See Table 4.

by reversing flow direction, especially when the standard process is operated in upflow mode at low Reynolds number, and close to the critical pressure of CO_2. The extent of natural convection can be roughly ascertained from the Grashof number for mass transfer. Gr is defined in terms of the cube of the particle diameter and solvent properties, i.e., the kinematic viscosity and the density gradient across the boundary layer. Consequently, Gr tends to be important for particles of large diameter or when the solute has a high solubility, leading in this case to significant density differences. Since kinematic viscosity is very small near the critical point, values of Gr are greater than those for heat transfer. Based on literature data (Knaff and Schlünder 1987; Lee and Holder 1995; Lim et al., 1990) and on the present results, free convection mass transfer should generally be considered as a further mechanism to transport. The lower limit of Grashof numbers where this may occur is $Gr > 10^7$ or $GrSc > 10^8$. A few well-defined experimental runs, upflow and downflow, are recommended to quantitatively assess the importance of free convection effects and whether or not the overall efficiency (total extraction time) of the entire process can be improved.

Effect of Particle Size. DCB extraction data for large pellets were also studied at $T = 313$ K and $P = 20$ MPa to see the influence of flow rate and flow direction on extraction rate. The data are not graphically represented, but the effect of particle size on K_G' is given in Figure 8b. For comparison, two runs using large and small pellets at $Re \approx 40$ and the downflow mode are illustrated in Figure 7.

At constant Reynolds number, the initial extraction rate is found to be only 3 times lower for the large pellets, although the interfacial area is 5 times less than

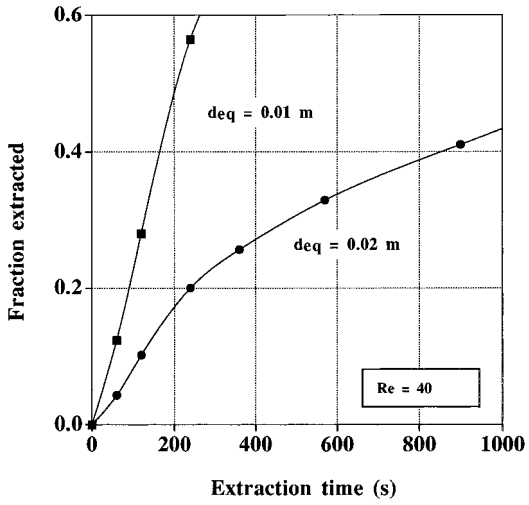

Figure 7. Effect of pellet size on the extraction rate of DCB at 20 MPa, 314 K.

that for the small pellets. This result suggests that the positive influence of natural convection is more important in the case of large pellets, for which the calculated Grashof numbers are 1 order of magnitude higher ($\approx 10^9$). In turn, internal diffusion affects the entire process more, resulting in total extraction times about 4−5 times longer than that for small pellets, but this aspect will not be discussed here.

Further evidence for the importance of natural convection is given by the change in the initial extraction rate with flow rate and flow direction. In the case of gravity-opposing operation, the initial slopes were very sensitive to flow rate as much as for small pellets. In the case of gravity-assisting flow, extraction rates appear to be independent of flow rate (see Figure 8b). Nevertheless, K_G' for extraction is larger for gravity-assisting flow in the range of low Reynolds numbers ($Re = 10-50$) (see Figure 8b).

Correlating Mass-Transfer Data

Mass-Transfer Coefficients. Values of K_G' were evaluated from eq 3, using experimental data and substance properties at corresponding operating conditions. The results of K_G' as a function of Re are given in Figure 8 for different systems and operating parameters. The figure shows that our K_G' values lie within the range $10^{-6}-10^{-4}$ m/s commonly encountered in SCF operations (Puiggené, 1996). As already pointed out, the strong variation of K_G' with Reynolds number results in a larger exponent for Re, about 0.7−0.9, for gravity-assisting and -opposing flows, respectively (see Figure 8a). The almost linear dependence on gas velocity suggests that the main mass transfer resistance is restricted to the SCF phase. Also, mass-transfer coefficients are greatly enhanced by natural convection effects at low Reynolds number (see Figure 8b and c). Downflow operation data at the particular conditions of 8 MPa and 313 K (small pellets) and at 20 MPa and 325 K (large pellets), respectively, indicate only a slight dependence on Re, which means that, here, mass transfer due to natural convection is dominant. Similar results near the critical point of carbon dioxide have been observed by different authors (Lim et al., 1990, Knaff and Schlünder, 1987). The influence of natural convection tends to vanish as the Reynolds number is increased (see Figure 8b and c), as reported in the studies of Lim et al. (1990, 1994) and us (Puiggené, 1996). Finally, it should be pointed out that K_G'

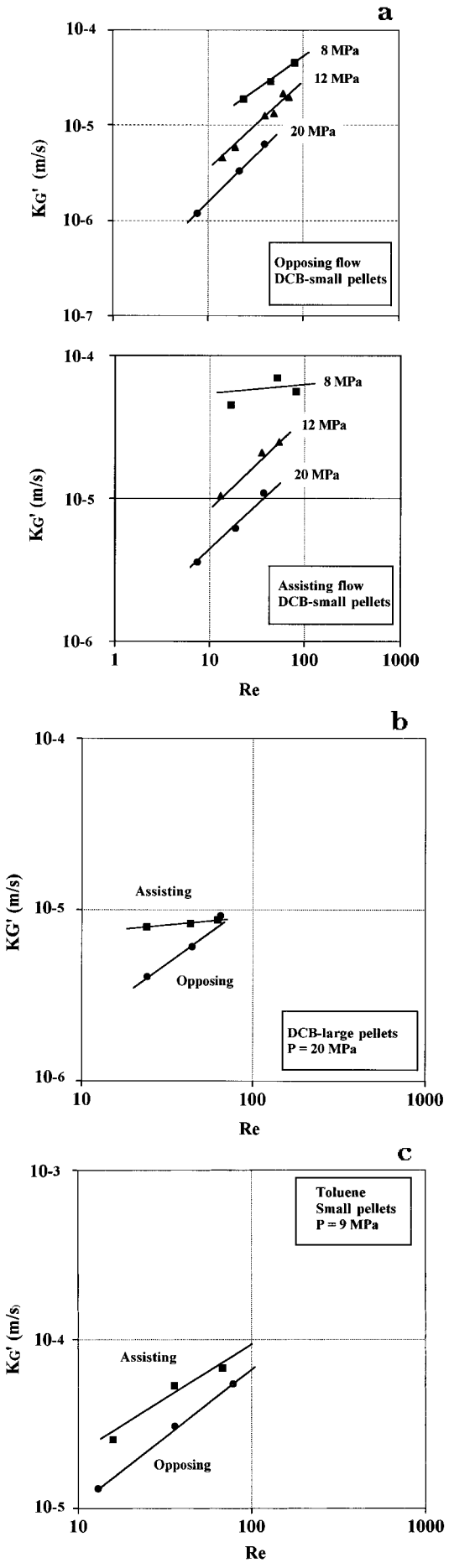

Figure 8. Mass-transfer coefficients vs Reynolds number for both upflow and downflow operation and (a) DCB/small pellets, (b), and (c) toluene/small pellets.

decreases with pressure at constant temperature, as expected from the effect of pressure on the gas-side mass-transfer coefficients found in the literature.

Mass-Transfer Correlations. Due to the behavior of our particular system under supercritical conditions, difficulties may arise in correlating mass-transfer data. Correlations for SC mass-transfer coefficients should differ from those for solid−gas or solid−liquid systems, in view of the values of the Schmidt number for gases at low pressure ($Sc \approx 1$) and for liquids ($Sc \approx 1000$). As noted above, the values of Gr numbers indicate that free convection intrudes in SCF mass-transfer mechanisms. In general, mass transfer between a saturated solution at the fluid−solute interface and the bulk solvent is the result of the superposition of three different mechanisms (Lim et al., 1990): molecular diffusion, free convective transport, and forced convection. Is is clear, in principle, that all three modes of transfer mechanisms have to be accounted for in the present study.

In this context, semiempirical models have been developed to include the different mechanisms in expressions based on dimensionless numbers such as

$$Sh = f(Re,Sc,Gr) \tag{4}$$

Depending on the experimental conditions, the following three cases are treated in the literature.

Pure Forced Convection. When forced convection is dominant, Grashof numbers are usually disregarded, and the general expression reduces to

$$Sh_F = Sh_0 + ARe^m Sc^p \tag{5}$$

where Sh_0 accounts for mass transfer due to molecular diffusion in the radial direction from the pellet. Both theoretical and empirical work done by Churchill and Churchill (1975) provides values for $Sh_0 = 0.68$ or 1 for cylinders for the heat-transfer analogue problem. Mills (1992) recomended $Sh_0 = 0.3$.

The coefficient A is a system parameter and depends on the geometry of the packing and flow configuration. Thus, $A = 0.13$ (Zehnder and Trepp, 1993), $A = 0.38$ (Tan et al., 1988), $A = 0.35$ (Steinberger and Treybal, 1960), $A = 1.1$ (Wakao and Kaguei, 1982). The theoretical Froessling value is 0.552. According to the laminar boundary layer theory, m and p are fixed to $m = {}^1/_2$ and $p = {}^1/_3$. For low-pressure gases, it is generally accepted by most authors that the variation in the exponent of Re is small ($m = 0.4-0.6$). At SC conditions, however, there exist cases where m is found to be much larger. In this regard, Tan and co-workers (1988) reported a value for m between 0.8 and 0.9. Brunner (1985) published a dependency larger than unity in the stripping of ethanol with dense CO_2 in a bubble column. Also, Bernad et al. (1993) observed a linear dependence on velocity for the fluid-side mass-transfer coefficient in a downflow trickling column with SC CO_2.

Pure Natural Convection. In the natural convection regime, the Reynolds number is unimportant, and the following expressions for the contribution to the Sherwood number have been suggested:

$$Sh_N = Sh_0 + b(ScGr)^{1/4} \tag{6}$$

for laminar free convection flow, i.e., $ScGr < 10^8$, and

$$Sh_N = Sh_0 + c(ScGr)^{1/3} Sc^{0.244} \tag{7}$$

for turbulent free convection flow, i.e., $ScGr > 10^8$.

The relation for turbulent natural convective flow is that suggested by Steinberger and Treybal (1960) and valid for heat and mass transfer to single spheres immersed in bounded and free-jet streams of gases and liquids at low pressures. It contains $Sc^{0.244}$ as a factor in the second term which is normally omitted in heat-transfer correlations. Steinberger found it necessary to separate data according to whether *Gr* was greater than 10^8, attributing this effect to the onset of a turbulent boundary layer in the higher range above 10^8. Values of *b* proposed in the literature range from 0.470 to 0.563. Available data for *c* are more different ($c = 0.0254$ from Steinberger−Treybal (1960) to $c = 0.112$ from Karabelas et al. (1971)) probably due to using different forms of eq 7.

Regime of Mixed Free and Forced Convection. In the present investigation, both natural and forced convection are important in global mass transfer. Forced convection is assumed to be laminar, according to the value of the Reynolds number (8−90) with respect to the limits given in Lim et al. (1990) and based on the work of Jolls and Hanratty (1965) and Karabelas et al. (1971). These authors observed that the transition of laminar to turbulent flow in packed beds occurs at $Re = 90-120$ and $Re = 110-150$, respectively. On the other hand, natural convection currents should be turbulent since the Rayleigh numbers for mass, $Ra = GrSc$, are calculated to be 10^8-10^{10} in our conditions and are far beyond the value for onset of the turbulent boundary layer, as given by Steinberger and Treybal (1960).

In order to combine natural and forced convection, most authors in the SCF field suggest using the heat-transfer correlating equation developed in terms of Nusselt numbers for free and forced convective heat transfer by Churchill (1977) but instead used in terms of Sherwood numbers (Knaff and Schlünder, 1987; Lim et al., 1990, 1994; Lee and Holder, 1995; Puiggené, 1996). In this case, the superposition rules are

$$Sh_T^{\,n} = Sh_F^{\,n} \pm Sh_N^{\,n} \tag{8}$$

and if the relations of Sh_F and Sh_N include molecular terms, Sh_0, a suitable form of eq 8 is (Mills, 1992)

$$(Sh_T - Sh_0)^n = |(Sh_F - Sh_0)^n \pm (Sh_N - Sh_0)^n| \tag{9}$$

where the subscripts T, F, and N indicate total, forced, and natural, respectively. The exponent *n* is a simple number as discussed below. As to the ± sign in eq 8, plus is for assisting flows and minus for opposing flows.

To eliminate the possibility of a zero total Sherwood number, Lim et al. (1990, 1994) and Lee−Holder (1995) developed a modified eq 8 to obtain a more complex relation as

$$Sh_T = ASh_F^{\,B} + C|Sh_F^{\,n} \pm DSh_N^{\,n}|^{1/n} \tag{10}$$

where *A*, *B*, *C*, *D*, and *n* are constants.

This type of equation may be more appropriate to use when natural convection is important and Sh_F and Sh_N are very close to each other, with the extractor operated in the gravity-opposing flow mode.

Concerning the value of the exponent *n*, Churchill (1977) selected 3 as an optimal value based on empirical correlation of experimental heat transfer data for the case of assisting flows. Although Lim et al. (1990) cite authors who support that there is a theoretical basis for $n = 3$, it is prudent to take *n* as a fitted exponent as done in Lee−Holder's eq 11. According to Mills (1992), for heat transfer by free convection *n* can take values between $n = 1$ and $n = {}^7/_2$, depending on geometry. Steinberger and Treybal (1960) postulated a simple additivity ($n = 1$) in eq 8, and Lee−Holder (1995) recently optimized *n* to a value of 0.6439 for their experimental data. We feel that this sole fact expresses that the total Sherwood number is relatively insensitive to the exponent *n* in the combination rule. Some confirmation is given by Churchill, who found that changing the optimal value of $n = 3$ to 2 or 4 involved only a small deviation of 10−20% at most.

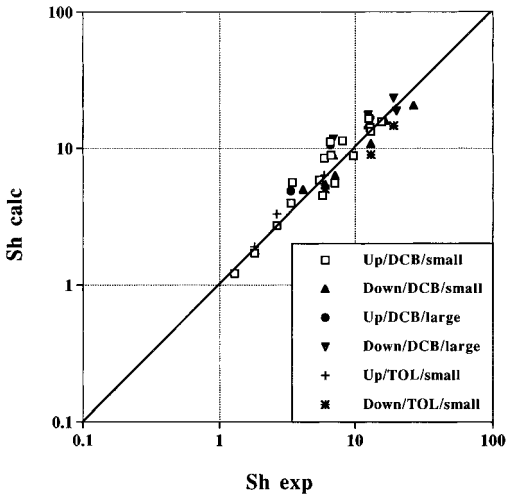

Figure 9. Comparison of predicted vs experimental mass-transfer data using the final correlation.

To correlate all present experimental data, the expressions given by eqs 5−7 for forced and natural convection will be used as a basis. Also, values of *n* from 1 to 4 were checked to see its effect on the goodness of fit. Using estimated substance properties, the expressions with $n = 1$ correlated best the experimental mass-transfer coefficients over the whole range of conditions studied. The parity plot for predicted vs observed Sherwood numbers is given in Figure 9. In summary, the correlations recommended are

$$Sh_T - Sh_0 = |Sh_F \pm (Sh_N - Sh_0)| \tag{11}$$

With $Sh_0 = 0.3$ (Mills, 1992), the correlations for natural and forced convection are

$$Sh_N = Sh_0 + 0.001(ScGr)^{0.33}Sc^{0.244} \tag{12}$$

$$Sh_F = 0.269Re^{0.88}Sc^{0.3} \tag{13}$$

for the following ranges of dimensionless numbers: $8 < Re < 90$, $3.5 \times 10^7 < GrSc < 10^9$, and $1.5 < Sc < 10$ with an AARD = 18.9%.

An advantage over similar mass-transfer correlations published to date is that a single set of parameters predicts mass transfer for gravity-opposing natural convection (with the minus sign in eq 11) as well as gravity-assisting natural convection (with plus sign in eq 11)). A better fit can be obtained with two separate equations, one for assisting and another for opposing flows, as pointed out by Lim et al. (1994). Differences in parameters and the gain in AARD being very small does not justify using two separate correlations given the simplicity of eqs 11−13 and the precision usually required in engineering work. On the other hand, changing the exponent *n* produces relatively larger deviations in the prediction of data. Thus, for $n = 2, 3,$

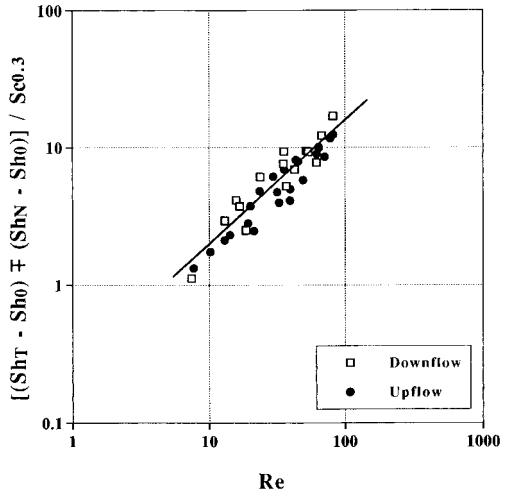

Figure 10. Contribution of forced convection to total mass transfer rate for all the runs (with toluene, DCB, small pellets, large pellets, upflow and downflow operation).

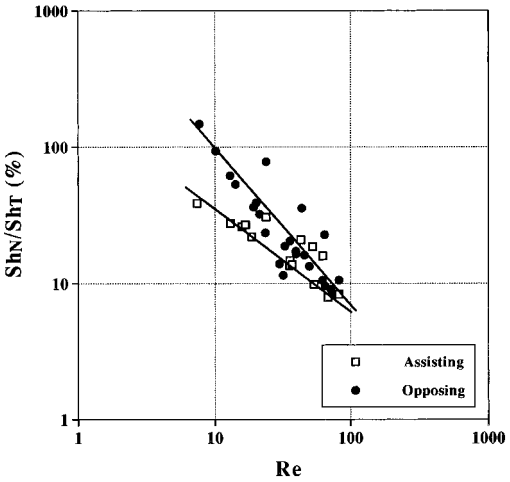

Figure 11. Contribution of natural convection as a function of Reynolds number.

and 4, the values of the AARD are 25%, 29.8%, and 30.2%, respectively ($Sh_0 = 0.3$).

For the purpose of graphically viewing of the correlation developed, a log−log plot of $|(Sh_T - Sh_0) \mp (Sh_N - Sh_0)|/Sc^{0.3}$ vs Re is shown in Figure 10 for all data of this study. This mode of plotting reduces the experimental data points to a natural convection-free basis, only depending on the Reynolds number. The solid line of Figure 10 corresponds to eqs 11−13, with an exponent of 0.88 on the Reynolds number as written in eq 13. The experimental data show a very good agreement with the final correlation (see Figure 10). Figure 11 shows the contribution of natural convection to the total Sherwood number as a function of the Reynolds number. As expected, Re numbers below 10 correspond to transport dominated by natural convection. But for Re around 90, still 10% of transport is due to natural convection (for both assisting and opposing flows).

A final evaluation of the present data is to test our correlation against the mass-transfer correlations available in the literature (for a short review, see Puiggené (1996)) under the operating conditions studied. Figure 12 illustrates a comparison of our own experimental results at $T = 313$ K and $P = 20$ MPa for the upflow extraction of DCB from the small pellets. In general, the order of magnitude of our data is lower than that observed for packed beds of solids (Lim et al. (1989, 1990) for solid naphthalene and Tan et al. (1988) for solid β-naphthol). It is interesting to see that the

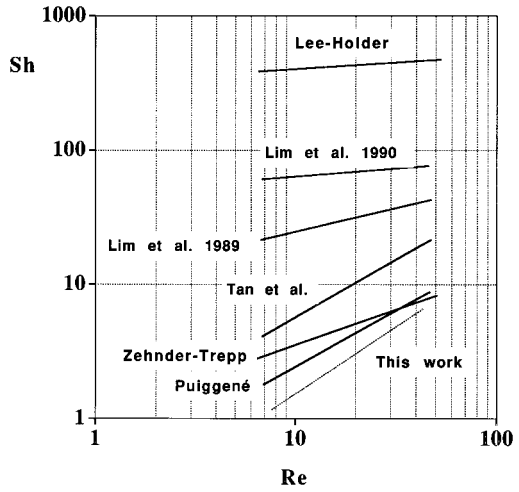

Figure 12. Comparison of Sherwood number for the mass transfer coeffcients measured in this work with existing correlations (upflow operation). $P = 20$ MPa, $T = 313$ K.

correlation of Lee and Holder (1995) gives quite high values, although being based on the data of Lim et al. (1989, 1990, 1994). The calculated values for the total Sherwood number are as much as 6−7-fold higher (see Figure 12) than those previously published by the Holder group (Lim et al., 1990). These rather surprising differences can be explained as follows. For the high Gr numbers of our study (Gr about 10^8−10^9), the correlations of Lee−Holder and Lim et al. give values that reduce to the case of pure natural convection flow. When the effect of the Reynolds number is small, the expressions take the forms

$$Sh_T \approx Sh_N = 0.309(ScGr)^{1/4} \quad \text{(Lim et al., 1990)} \tag{14}$$

$$Sh_T \approx Sh_N = 2.175(ScGr)^{1/4} \quad \text{(Lee−Holder, 1995)} \tag{15}$$

It is remarkable that the coefficient in front of the second equation (2.175) is approximately 7 times that of the first equation (0.309), thus exactly reflecting the differences of Figure 12.

Not unexpectedly, the correlations developed when a liquid−fluid interface is present (Zehnder and Trepp, 1993; Puiggené, 1996) lie near those developed here. In an earlier paper, we reasoned that an additional mass-transfer resistance could be present in the liquid film in contact with the SCF, due to the large solubility of the high-pressure gas in the liquid. This would explain the lower Sh number for the bottom lines of Figure 12. The hypothetical effect of capillary drying (Barton et al., 1993) could contribute to mass transfer to the fluid in all liquid−fluid systems.

Conclusions

External, particle-to-fluid mass-transfer coefficients of 1,2-dichlorobenzene and toluene in supercritical carbon dioxide were measured over ranges of 8−20 MPa and 310−360 K in packed beds. Sintered metallic pellets of two different sizes were employed as inert solid packings. The analysis of the curves of extracted mass vs time yielded reproducible results suitable to establish volumetric mass-transfer coefficients. In particular, the slopes of the mass vs time curves at vanishing extraction time could be used to determine mass-transfer coef-

ficients, as the initial extraction rates are not limited by intraparticle diffusion. Extraction with SC CO_2 was found to be affected by pressure, temperature, fluid velocity, pellet size, and flow direction.

The measurements were performed in the ranges of $Re = 8-90$ and $GrSc = 10^8-10^{10}$. Therefore, the ratio of buoyant to inertial forces is significant, and the free convection mechanism was suspected to contribute to the global mass-transfer rates. This was experimentally verified by performing the same runs with upflow and downflow of fluid. For example, at conditions near the critical point, the extraction time for 50% recovery of solute with gas flowing against gravity (opposing flow) almost tripled the time for the same recovery with downflow of fluid (assisting flow).

On the other hand, the measured mass-transfer coefficients for both upflow and downflow operation exhibited a significant dependence on the Reynolds number. Therefore, in order to correlate mass-transfer data, it seemed appropriate to use an equation which accounts for mass transfer due to mixed free and and forced convection. An equation in which the total Sherwood number is a linear algebraic sum of the Sherwood numbers for free and forced convection provided satisfactory results. The developed single correlating equation, with one set of optimized parameters and only one change in a sign, predicts well mass transfer for both gravity-opposing flow and gravity-assisting flow.

Acknowledgment

This work was done with the economic support of the Spanish Ministry of Education and Science through Grant Number AMB95-0042-C02-02 (CICYT, Madrid). We appreciate the interest and help of AMES (Barcelona) for supplying standard analytical methodologies for sintered metallic parts as well as pellet samples. A SGR 95 fellowship received from CIRIT (Generalitat de Catalunya, Barcelona) is gratefully appreciated.

Nomenclature

a = external area of packing per unit bed volume, m^{-1}
a_{eff} = effective specific external area of packing per unit bed volume, m^{-1}
C_G = concentration of solute in fluid phase, mol/m^3
C^*_G = concentration of solute in fluid phase at saturation, mol/m^3
D = molecular diffusivity, m^2/s
d_{eq} = equivalent particle diameter, m
d_p = particle diameter, m
G = mass flow rate, $kg/(m^2\ s)$
Gr = Grashof number, $Gr = [(d_p^3 g)/\nu](\Delta\rho/\rho)$
$K_G' = K_G(a_{eff}/a)$, s^{-1}
K_G = overall gas phase mass transfer coefficient based on an effective area, a_{eff}, m/s
m = weight of solute, kg
M_{solute} = molecular weight of solute, kg/mol
P = pressure, MPa
Ra = Rayleigh number, $Ra = GrSc$
Re = Reynolds number, $Re = Gd_{eq}/\mu$
Sc = Schmidt number, $Sc = \nu/D$
Sh = Sherwood number, $Sh = K_G' d_{eq}/D$
T = temperature, K
t = time, s
v_{SCF} = linear velocity at high pressure, m/s
V = bed volume, m^3
X = extracted mass fraction of solute
Y^* = solubility expressed in mole fraction, mol/mol

Greek Letters

θ_{pellet} = internal porosity of pellet
μ = dynamic viscosity, Pa s
ρ = density, kg/m^3
$\Delta\rho = \rho^* - \rho$, kg/m^3
ρ^* = density of saturated solution, kg/m^3
ν = kinematic viscosity, m^2/s

Appendix

During this work, methods were required for evaluating solubilities in SC CO_2 and other thermophysical and transport properties (CO_2 density, densities of saturated solutions, viscosities, and diffusivities). These were necessary for calculating the Reynolds, Grashof, Schmidt, and Sherwood numbers. Material data are summarized in Table 3 for the conditions of the experimental runs. The density of pure carbon dioxide was calculated with the Bender equation of state as given by Knaff and Schlünder (1987). The saturated mixture density at given system conditions was determined with the Peng and Robinson (1976) equation of state for mixtures, together with solubility data as shown later. The binary interaction parameter, k_{12}, for DCB−CO_2 was 0.1275, calculated from the VLE data of Puiggené (1996) (see below). For the system toluene−CO_2, k_{12} is 0.077 51 (Brown et al., 1987). The viscosity of mixtures was approximated by that of pure CO_2 and calculated by the Reichenberg (1975) correlation using the low-pressure viscosity determined from the Chapman−Enskog theory. Further material properties such as binary diffusivities for DCB and toluene in CO_2 were determined from the correlation of Catchpole and King (1994). Their method was specially developed for various solvent and solutes at supercritical conditions. For the toluene−CO_2 system, diffusivities reported by Lee and Holder (1995) and our estimates agreed well. As eq 2 indicates, the mass-transfer coefficient is inversely proportional to solubility. Therefore, the quality of the calculated mass-transfer coefficients depends on the accuracy of solubilities. We thus give a detailed account on how solubilities were established. The calculation of solubility of DCB in SC CO_2 is based on the experimental values of the liquid−fluid partition coefficient, K^{exp}, defined as the ratio of the equilibrium molar concentrations:

$$K = \frac{C^*_G}{C_L} \tag{A1}$$

In an ealier work in our laboratory (Puiggené, 1996), we studied the evaporation of DCB as a free liquid into SC CO_2 from a bed of impermeable spheres. We fitted simultaneously a mass-transfer coefficient and the partition constant, K, using a well-mixed flow model for the extractor. Values of K^{exp} are given in Table 2 for $T = 310$ K and $P = 8-25.5$ MPa. If critical constant and acentric factors for pure substances are known, it is possible to solve the VLE and, thus, determine the gas and liquid equilibrium concentrations required to evaluate the partition constant K^{theo} using eq A1. The Peng−Robinson equation of state with the mixing rules of Panagiatopulos and Kumar (Reid et al., 1987) is selected for calculations. For the system DCB−CO_2, no value of the interaction parameter, k_{12}, is available in the literature, and an estimate is not suitable due to the extreme sensitivity of the solubility to k_{12} (Brunner, 1995). The procedure was to optimize k_{12}, in order to fit the measured K^{exp} values (see Table 2). The value of $k_{12} = 0.1175$ used in this study is slightly smaller than that given by Puiggené (1996) but gives a better

global fit over the entire pressure range (Table 2). The solubility of DCB in SC CO_2 appears to be high, somewhat higher than those for solid naphthalene. For the system toluene−CO_2, Fink and Hershey (1990) experimentally characterized the VLE using the Peng−Robinson EOS. The interaction parameter value $k_{12} = 0.077\ 51$ of Brown et al. (1987) agrees well with the Fink and Hershey values. SC CO_2 is a good solvent for toluene. However, a different behavior is noted for the critical pressure of the mixture. Thus, for DCB−CO_2, the critical pressure is around 30 MPa and about 10 MPa for the system toluene−CO_2.

Literature Cited

Barton, P.; Hughes, R. E.; Hussein, M. M. Supercritical Carbon Dioxide Extraction of Pepermint and Spearmint. *J. Supercrit. Fluids* **1992**, *5*, 157.

Barton, P.; Shah, S.; Fulkerson, W. C. Supercritical Fluid Extraction of Binders in Processing of Ceramic. *Prepr. Pap., Natl. Meet.—Am. Chem. Soc.* **1993**, *33*, 371.

Bernad, L.; Keller, A.; Barth, D.; Perrut, M. Separation of Ethanol from Aqueous Solutions by SC Carbon Dioxide. *J. Supercrit. Fluids* **1993**, *6*, 9.

Beutler, H. J.; Gährs, H. J.; Lenhard, U.; Lürken, F. Einfluβ der Lösungsmittelführung auf den Hochdruck-Extraktions-Prozeβ. *Chem.-Ing.-Tech.* **1988a**, *60*, 773.

Beutler, H. J.; Lenhard, U.; Lürken, F. Erfahrungen mit der CO_2 Hochdruckextraktion auf dem Gebiet der Fettextraktion. *Fats Sci. Technol.* **1988b**, *90*, 550.

Brennecke, J. F.; Eckert, C. A. Phase Equilibria Gas Supercritical Fluid Processing. *AIChE J.* **1989**, *35*, 1459.

Brown, B. O.; Kishbaugh, A. J.; Paulauitis, M. E. Experimental Determination of Enhancement Factors from Supercritical-Fluid Chromatography. *Fluid Phase Equilib.* **1987**, *36*, 246.

Brunner, G. In *Mass Transfer in Gas Extraction in Supercritical Fluid Technology*; Penninger, J.M.L., Radosz, M., McHugh, M. A., Eds.; Elsevier: Amsterdam, 1985.

Brunner, G. *Dense Gas Extraction*, Springer Verlag: Berlin, 1995.

Catchpole, O. J.; King, M. B. Measurement and Correlation of Binary Diffusion Coefficients in Near Critical Fluids. *Ind. Eng. Chem. Res.* **1994**, *33*, 1828.

Churchill, S. W. A Comprehensive Correlation Equation for Laminar, Assisting, Forced and Free Convection. *AIChE J.* **1977**, *23*, 10.

Churchill, S. W.; Churchill R. U. A Comprehensive Correlation Equation for Heat and Component Transfer by Free Convection. *AIChE J.* **1975**, *4*, 604.

Debenedetti, P; Reid, R. C. Diffusion and Mass Transfer in Supercritical Fluids. *AIChE J.* **1986**, *32*, 2034.

Fink, S. D.; Hershey, H. C. Modeling the VL Equilibria of 1,1,1-Trichloroethane + Carbon Dioxide and Toluene + Carbon Dioxide at 308, 323 and 353 K. *Ind. Eng. Chem. Res.* **1990**, *29*, 295.

Jolls, K. R.; Hanratty, Y. J. *AIChE J.* **1965**, *15*, 199.

Jones, M. C. Mass Transfer in SCFE from Solid Matrices. In *Supercritical Fluid Technology*; Bruno, T. J., Ely, J. F., Eds.; CRC: Boca Raton, FL, 1991.

Karabelas, A. J; Wegner, T. H.; Hanratty, T. J. Use of Asymptotic Relations to Correlate Mass Transfer Data in Packed Beds. *Chem. Eng. Sci.* **1971**, *26*, 1581.

Kelley, F. D.; Chimowitz, E. H. Near Critical Phenomena in Supercritical Fluid Chromatography. *AIChE J.* **1990**, *36*, 1163.

Knaff, G.; Schlünder, E. U. Mass Transfer for Dissolving Solids in Supercritical Carbon Dioxide. Part I: Resistance of the Boundary Layer. *Chem. Eng. Process.* **1987**, *21*, 151.

Lee, C. H.; Holder, G. D. Use of Supercritical Fluid Chromatography for Obtaining Mass Transfer Coefficients in Fluid−Solid Systems at Supercritical Conditions. *Ind. Eng. Chem. Res.* **1995**, *34*, 906.

Lim, G.-B; Holder, G. D.; Shah, Y. T. Solid−Fluid Mass Transfer in a Packed Bed under Supercritical Conditions. In *Supercritical Fluid Science and Technology*; Johnston, K. P., Penninger, J. M. L., Eds.; ACS Symposium Series 406; American Chemical Society: Washington, DC, 1989.

Lim, G.-B.; Holder, G. D.; Shah, Y. T. Mass Transfer in Gas−Solid Systems at Supercritical Conditions. *J. Supercrit. Fluids*. **1990**, *3*, 186.

Lim, G. B.; Shin, H. Y.; Noh, M. J.; Yoo, K. P.; Lee, H. *Subcritical to Supercritical Mass Transfer in Gas Solid System*; Brunner, G., Perrut, M., Eds.; Proceed. 3rd. Intl. Symp. Supercrit. fluids. ISASF: Strasbourg, 1994.

Madras, G.; Thibaud, C.; Erkey, C.; Akgerman, A. Modeling of Supercritical Extraction of Organics from Solid Matrices. *AIChE J.* **1994**, *40*, 777.

McHugh, M. A.; Krukonis, V. *Supercritical Fluid Extraction—Principles and Applications*, 2nd ed.; Butterworths: Boston, 1994.

Mills, A. F. *Heat Transfer*; Irwin: Boston, 1992.

Peng, D.-Y.; Robinson, D. B. A New Two-Constant Equation of State. *Ind. Eng. Chem. Fundam.* **1976**, *15*, 59.

Puiggené, J. Ph.D. Thesis (in progress), UPC Barcelona, 1996.

Recasens, F.; McCoy, B. J.; Smith, J. M. Desorption Processes: Supercritical Fluid Regeneration of Activated Carbon. *AIChE J.* **1989**, *35*, 951.

Recasens, F.; Velo, E.; Larrayoz, M. A.; Puiggené, J. Endothermic Character of Toluene Adsorption from Supercritical Carbon Dioxide on Carbon at Low Coverage. *Fluid Phase Equilib.* **1993**, *90*, 265.

Reichenberg, D. New Method for the Estimation of the Viscosity Coefficients of Pure Gases. *AIChE. J.* **1975**, *21*, 1811.

Reid, R. C.; Prausnitz, J. M.; Poling, C. E. *The Properties of Gases and Liquids*, 4th ed.; McGraw-Hill: New York, 1987.

Sovová, H.; Kucera, J.; Jez, J. Rate of the Vegetable Oil Extraction with Supercritical CO_2—II. Extraction of Grape Oil. *Chem. Eng. Sci.* **1994**, *49*, 415.

Steinberger, R. L.; Treybal, R. E. Mass Transfer from a Soild Soluble Sphere to a Flowing Liquid Stream. *AIChE J.* **1960**, *6*, 227.

Tan, C. S.; Liou, D. C. Desorption of Ethyl Acetate from Activated Carbon by Supercritical Carbon Dioxide. *Ind. Eng. Chem. Res.* **1988**, *27*, 988.

Tan, C. S.; Liang, S. K.; Liou, D. C. Fluid−solid Mass Transfer in supercritical Fluid Extractor. *Chem. Eng. J.* **1988**, *38*, 17.

Wakao, N.; Kaguei, S. *Heat and Mass transfer in Packed Beds*; Gordon and Breach: New York, 1982.

Zehnder, B; Trepp, Ch. Mass-Transfer Coeffcients and Equilibrium Solubilities for Fluid-Supercritical-Solvent Systems by Online Near-IR Spectroscopy. *J. Supercrit. Fluids* **1993**, *6*, 131.

Received for review March 18, 1996
Revised manuscript received June 28, 1996
Accepted June 29, 1996[⊗]

IE9601514

[⊗] Abstract published in *Advance ACS Abstracts*, September 15, 1996.